Subsurface crack determination by one-sided ultrasonic measurements

D.G. Aggelis *, E. Leonidou, T.E. Matikas

Department of Materials Science and Engineering, University of Ioannina, 45110 Ioannina, Greece

ARTICLE INFO

ABSTRACT

Corrosion of steel reinforcement in concrete is a common type of damage. The cracks propagate from the steel bar to the surface without giving any visual sign prior to surface crack formation. As long as the surface material is intact, the sensitivity of the longitudinal wave velocity to the subsurface cracks is doubtful. In this paper, cracks were created in steel fiber reinforced concrete specimens by four point bending. Wave measurements took place on the intact surfaces (compression side) using common acoustic emission transducers. Although there was no visual sign of the crack, Rayleigh as well as longitudinal wave velocities clearly decreased relative to those of the sound material. Other parameters like the amplitude and the experimental scatter of the waves were much more sensitive to damage. Numerical simulations were conducted in order to make a parametric study concerning the depth of the sound layer, the propagating wavelength and the measured wave parameters and propose a firm methodology. It is concluded that by scanning a surface with simple acoustic one-sided measurements, the identification of the location of the subsurface damage is possible, while the propagating wave gives information about the depth of the crack.

1. Introduction

Surface damage is the most common type of damage in concrete. Repair of concrete structures is based on a preliminary visual inspection. When the cracks are visible from the surface, they can be targeted by one-sided measurements using longitudinal (P-waves) or Rayleigh waves for depth assessment [1,2]. However, when the defects are subsurface, they give no visual warning until they break the surface. This is the case for corrosion cracks starting from reinforcing steel bars. The layer of rust created on the metal surface applies additional stress to the surrounding concrete and cracks are nucleated [3]. These cracks propagate away from the steel bar (Fig. 1) and after breaking the surface the deterioration is accelerated by additional water or chemical agents which penetrate deep into the structure. Considering that the rebars are usually embedded several cm (in) inside concrete, it should take several years before these cracks become visible. Therefore, nondestructive testing techniques for the estimation of the subsurface material quality are highly demanded [3]. The motivation for this study comes from a concrete bridge monitoring project [4]. Acoustic emission and ultrasonic monitoring demonstrated that a part of the bridge was severely deteriorated although there was no visual sign of damage. Thus it was reasonable to assume that the damage was subsurface and originated from the metal reinforcement which was embedded 50 mm inside the structure.

Ultrasonic properties, such as velocity and attenuation measured on the surface, may be influenced by subsurface damage, even though a shallow layer of the material remains intact. For Rayleigh surface waves it is accepted that the penetration depth is approximately equal to one wavelength [5]. For longitudinal waves though, the depth of propagation is not straightforward. Therefore, any specific P-wave velocity measured on the surface is characteristic of a layer of unknown thickness. Thus, the studies of interaction between elastic waves and surface-breaking or near surface cracks are of considerable interest in the field of quantitative non destructive testing (NDT) [6–11].

In the present study concrete prisms were subjected to 4-point bending. Cracks developed from the tensile bottom side to the top without breaking the specimen in two because the specimens were reinforced by steel fibers. After the bending experiment, ultrasonic one-sided measurements took place on the compression side that was still intact. Velocity, attenuation as well as experimental scatter parameters were studied using acoustic emission transducers. It is examined if the identification of sub-surface damage is possible using conventional equipment by simple sensor application on the surface. Additionally, the elastic wave problem is numerically simulated in order to verify the experimental trends and propose the most suitable experimental conditions (e.g. frequency) in order to have an efficient assessment.

2. Experimental details

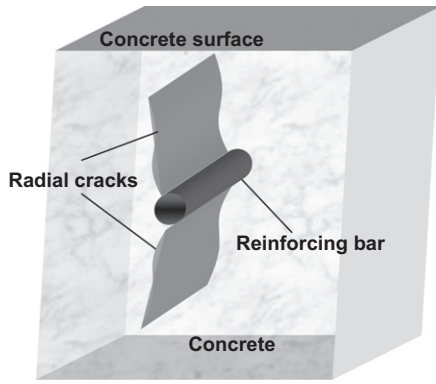The specimens used were made of steel fiber-reinforced concrete (SFC). Their size was 400 × 100 × 100 mm. The water to

---

* Corresponding author. Tel.: +30 26510 08006; fax: +30 26510 08054.
E-mail address: daggelis@cc.uoi.gr (D.G. Aggelis).

Fig. 1. Development of subsurface cracks by corrosion of rebar.

Fig. 2. Snapshot of the bending experiment.

stopped at the mid span deflection of 2 mm according to the standard. However, it is clear that the actual crack shape could not be controlled. This would be possible only by inserting sheets when casting concrete. However, the sheets would differ significantly from actual cracks and therefore, it was decided to work on actual cracks that were produced for a mid span deflection of the specimens of 2 mm.

These specimens were used for one-sided wave measurements. The experimental setup for the elastic wave measurements is depicted in Fig. 3a. Two sensors were placed on the intact side of the specimen at a distance of 70 mm. The excitation was conducted by pencil lead break which introduces a frequency band approximately from 0 to 200 kHz. The sensors were common acoustic emission transducers (Physical Acoustics, PAC R6), with nominal sensitivity around 60 kHz, and diameter of 15 mm. The sampling frequency of the acquisition board was set to 5 MHz. Fig. 3b shows a snapshot during the experiment. This kind of ultrasonic set up is commonly used in monitoring of concrete structures [4,13].

Wave velocity was measured by the time delay between the waveforms collected at the different sensors. Typical waveforms recorded on sound material are depicted in Fig. 4a. For pulse velocity determination the first disturbance (wave onsets in Fig. 4a) was used. The onset corresponds to the longitudinal wave which is the fastest type. Rayleigh wave velocity was measured by its strong characteristic peak (see again Fig. 4a). Concerning the Rayleigh, it should be mentioned that their energy is much higher than any other type. A point source on a half space radiates 67% of its energy in the form of Rayleigh waves, while only 7% in compressional ones [7]. Moreover, since they are essentially two-dimensional, their energy does not disperse as rapidly as the energy associated with three-dimensional dilatational and shear waves [14]. Specifically, their amplitude is inversely proportional to the square root of propagation distance while for a longitudinal wave the amplitude is inversely proportional to the distance. This makes them more easily detectable than other kinds of waves even in longer distances [15]. Specifically, they are recognized by a strong peak after the initial longitudinal weak arrivals [5]. Additionally, their particle displacement is ellipsoidal with the out of plane vector approximately three times higher than the in plane, making them easily detectable by common P-wave transducers. Still, it is mentioned that in some cases with severe cracking it is difficult to discriminate the Rayleigh peak. However, this by it self shows that the crack has cut through the whole cross section. Fig. 4b shows typical waveforms for the case of a subsurface crack on a 1.5% fiber concrete. The waveform of the first receiver is similar to the sound case; however, the waveform recorded by the second waveform is much lower. The measurements were conducted twenty times by slightly translating and rotating the receivers' array around the crack in order to study also the experimental scatter for sound and cracked material. By changing the position of the receivers the wave was obtained through a random number of paths which is quite large (20 paths) considering the small surface of a few cm^2
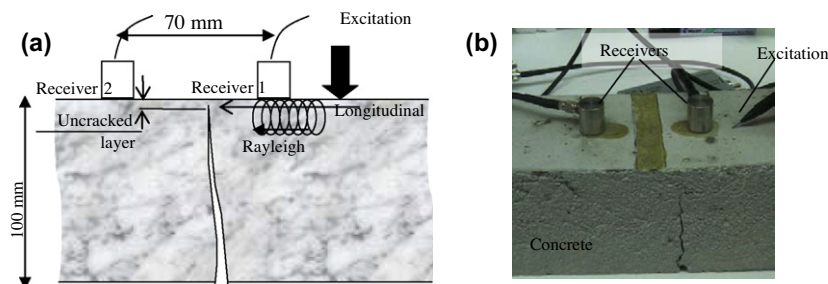
cement ratio by mass was 0.5 and the aggregate to cement ratio 5. The maximum aggregate size was 10 mm. Different fiber contents were applied, specifically 0.5%, 1% and 1.5% by volume. The fibers were undulated with length 25 mm and diameter 0.5 mm. Additionally, plain concrete specimens were cast. The specimens were tested in 4-point bending for fracture toughness determination (ASTM C1609/C 1609 M-05) resulting in vertical cracks which propagated from the bottom tensile surface to the top. The specimens did not split in two parts because of the fiber action. The plain specimen was not split as well but was handled with extreme care for the following measurements. Therefore, the top surface was intact but most of the specimens' cross section was ruptured (see Fig. 2). Although it is not within the subject of this study, it is mentioned that the maximum load withstood by the specimens was approximately 15 kN for plain concrete reaching 20 kN for the 1.5% fiber concrete. More details on the specimen's composition can be seen in another study [12]. The bending experiments were

Fig. 3. (a) Experimental setup for one-sided wave measurements and (b) snapshot of the wave measurement.
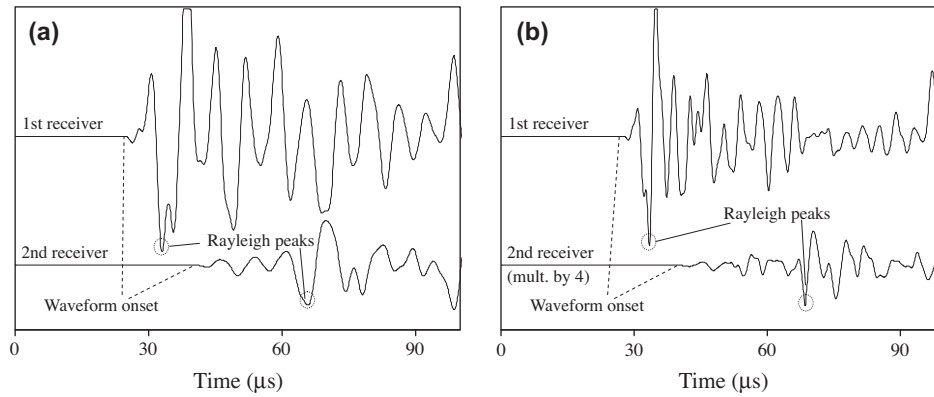
Fig. 4. Typical waveforms for (a) sound material and (b) subsurface cracked material.
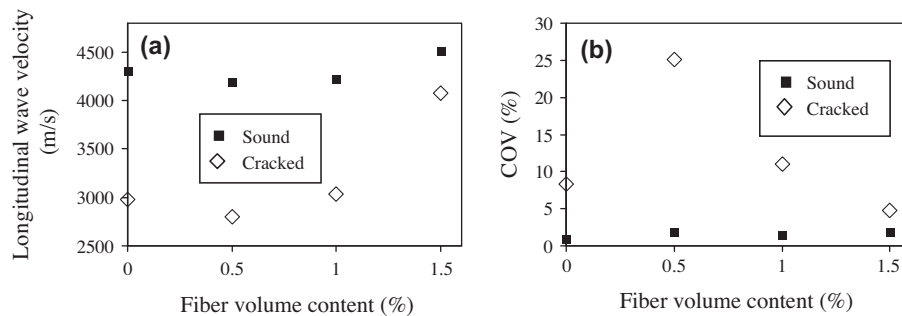

Fig. 5. (a) Pulse velocity for intact and cracked material for different fiber content and (b) COV of the results of (a).

around the crack. The additional measurements take just a few minutes which is a minimal time span when the equipment is set.

3. Longitudinal wave results

Fig. 5a shows the velocity of longitudinal waves for different fiber content. It is the average of the 20 measurements on each specimen. For the intact condition, plain concrete exhibits a velocity around 4300 m/s, while the velocity of concrete reinforced with 1.5% of fibers is higher than 4500 m/s. For 0.5% and 1% of steel fibers the velocity is slightly lower than that of plain concrete (approximately 4200 m/s), although steel is stiffer than concrete. Similar cases have been studied in literature showing that stiff inclusions do not necessarily increase the velocity of a softer matrix for any given frequency [16]. These phenomena are attributed to scattering and are beyond the scope of this paper. In any case, as long as intact material is concerned, the velocity is not much influenced by the fiber content. This implies that the existence of cracks should be easily highlighted.

For the case of subsurface cracks, the velocity decreases for all fiber contents (Fig. 5a). The decrease is clearer for low or no inclusion content, (more than 1000 m/s), while for the 1.5% fibers the decrease is about 500 m/s. The small decrease for heavily reinforced concrete is attributed to the extensive bridging of the crack faces by the fibers. The wave paths provided by the steel fibers allow a sufficient amount of energy to propagate through the crack and reach the receiver. Thus the velocity is measured to the level of sound concrete although the crack is located just a few mm below the surface. Therefore, for this case of heavily reinforced concrete, judging only from the value of velocity would not be safe to evaluate the actual condition. Bridging influences also the determination of surface breaking cracks, where any kind of filling

material (reinforcement, water, dust) would make one-sided measurements of longitudinal waves troublesome [9,17].

Fig. 5b shows the coefficient of variation (COV) of the total population of measurements (standard deviation divided by the average). For intact material, the variation is very low (1–2%). This is reasonable since the material is quite homogeneous and measuring different paths should result in the same velocity. This small deviation accounts for any experimental errors (i.e. sensor coupling), as well as the limited inhomogeneity of concrete itself which contains sand grains, small aggregates, fibers, porosity and air bubbles. On the other hand, when subsurface damage is present, the experimental scatter increases significantly, as seen again in Fig. 5b, even up to 25%. This implies that COV could be easily implemented in practice in order to improve characterization. In fact the coefficient of variation of a sufficient number of measurements has been correlated with damage content in surface wave measurements [18]. The reason is that changing the location of the sensors, changes also the location and orientation of the crack relatively to the wave direction. For example the width of the crack cannot be uniform in the whole thickness of the specimen, or for some wave paths, fibers or aggregates could bridge the two sides at some points and different heights. Therefore, each individual waveform is different as the wave propagates through a wave path with different characteristics. Consequently, it is reasonable that the measured parameters, like the velocity will also exhibit high experimental scatter compared to the values measured on sound material.

4. Rayleigh waves

The velocity of Rayleigh waves shows similar trends with longitudinal. Concrete with 1.5% fiber exhibits the highest velocity (more than 2300 m/s), while the lowest is exhibited by 0.5% (2150 m/s), as seen in Fig. 6a. For the cracked material the velocity
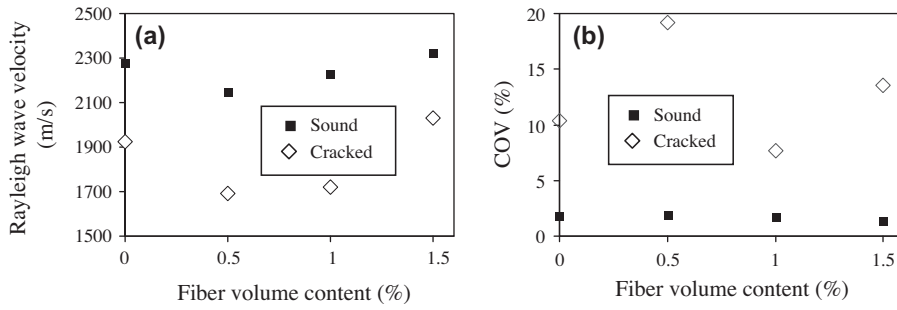
Fig. 6. (a) Rayleigh velocity for intact and cracked material for different fiber content and (b) COV of the results of (a).

decrease is clear. Velocity ranges from 1700 m/s (0.5% of fibers) to 2000 m/s (1.5% fibers). Again COV for sound material is less than 2% but increases to 8–20% for the cracked specimens as seen in Fig. 6b. From both longitudinal and Rayleigh waves it is evident that velocity decreases by about 20–25% compared to the intact material. However, the standard deviation of the measurements is increased at least 3–13 times being much more sensitive to the existence of damage. It is mentioned that in an actual situation metal rebars would be below the surface of concrete. However, they would not affect the readings since the wavelength used is quite short. Considering a mean frequency of 100 kHz excited by the pencil lead break, the Rayleigh wavelength is calculated at about 22 mm which is much shallower than the metal bar depth. Even if the wavelength was longer, still the great influence would be only when the bar is parallel to wave propagation (or the sensor array). Since many measurements are taken with different orientations, this effect would be minimized.

5. Amplitude

Wave velocity is certainly indicative of damage, but its sensitivity is limited. Even close to final failure, pulse velocity decreases by 10–20% [19]. However, energy or amplitude parameters decrease even from low levels of loading because they are more sensitive to inhomogeneity, even micro-cracking. Attenuation mechanisms are active even in intact material due to damping and geometric spreading. As the inhomogeneity increases, scattering becomes also an important mechanism [20]. In the present case the subsurface cracks reflect a large amount of energy of the wave, allowing propagation only through the thin intact layer or through the fibers bridging the crack sides. In order to quantify the results, the maximum absolute amplitude of the waveform of the second receiver was divided by the amplitude of the first to yield the percent surviving amplitude. It is mentioned that for damaged concrete it is not always easy to identify which is the wave type that carries the highest amplitude. This is why "waveform amplitude" is mentioned and not specifically Rayleigh or longitudinal. However, due

to many reasons mentioned earlier, the maximum amplitude of the wave should be attributed to the Rayleigh.

For the sound material, the surviving amplitude was approximately 30–37% (see Fig. 7a) for any content of fibers in concrete. This shows that the effect of fibers is weak and the influence of the cracks should not be masked. In case subsurface damage is present the surviving amplitude diminishes to 3–11% (see again Fig. 7a). Again, concrete with 1.5% of fibers exhibits the highest amplitude in the cracked state due to the bridging of the cracks. In any case amplitude proves to be a more reliable parameter than velocity since it decreases by about 90% compared to the healthy material, while as stated earlier, velocity suffers a decrease of approximately 25%. The inherent inhomogeneity of the material, which includes porosity, air bubbles, sand, aggregates and fibers increases the COV of the amplitude measurements even for the sound material since amplitude is more sensitive to inhomogeneity. Therefore, the existence of damage did not increase the COV of amplitude measurements as clearly as in the case of velocity (see Fig. 7b).

6. Numerical simulation

Simulations enhance our understanding in wave propagation. Cases which are difficult or costly to be examined experimentally can be studied through simulations. In the present case, the experiment was conducted by resonant sensors. Therefore, simulations are a way to expand to different frequencies. Additionally, although the bending experiments were conducted with deflection control, there was no control on the length of the subsurface cracks developed. These cracks almost reached the opposite surface and thus, had a clear effect on the wave parameters. In order to examine different cases of subsurface crack depths, numerical simulations were performed.

Simulations were conducted with commercially available software [21]. It operates by solving the two-dimensional elastic wave equations based on a method of finite differences and has been used recently for wave propagation in inhomogeneous concrete
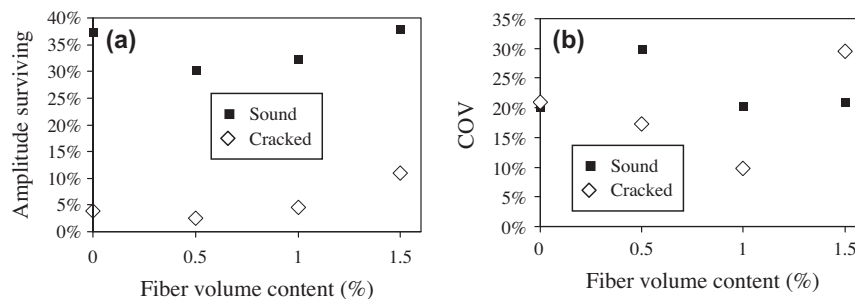

Fig. 7. (a) Waveform amplitude for intact and cracked material for different fiber content and (b) COV of the results of (a).

[22]. The material was considered elastic with no viscosity components. The Lame constants were λ = 12 GPa and μ = 16.5 GPa, with density of 2400 kg/m³, resulting in a longitudinal wave velocity of 4300 m/s. The corresponding Elastic modulus is 40 GPa and Poisson's ratio 0.2. Concrete is by definition inhomogeneous. The aggregates and sand certainly induce some scattering on the propagating wave. However, due to their similar mechanical impedance to the mortar matrix (similar elastic modulus and density) the scattering will be negligible compared to the scattering on an actual crack, which exhibits zero density. Due to the severe mismatch the crack will block most of the energy, while the aggregates have not such a strong effect. Additionally, fibers which are critical for the fracturing behavior of the material, are insignificant for wave scattering effects since their thickness is negligible compared to the applied wavelengths. This is the reason, concrete was considered homogeneous with the above mentioned properties.

The geometric model was of rectangular shape with 100 mm thickness to resemble the experimental specimen, see Fig. 8a. The spacing resolution (spacing of the finite difference grid) of calculation was set to 0.2 mm much smaller than the longitudinal wavelength of 43 mm, as well as the Rayleigh of 24 mm ensuring accurate solution. In order to reduce the calculation time, the specimen length was reduced to 200 mm and infinite boundary conditions were applied to the opposite sides, cancelling the reflections from the edges. The two simulated receivers were 15 mm long to resemble the actual transducers and were placed on the top side of the specimen with a separation of 70 mm. The receivers computed the average lateral displacement on their defined length. The simulated cases, concerned the crack-free geometry as well as geometries with subsurface cracks. The intact layer between the surface and the crack was varied, namely at 60 mm, 40 mm, 20 mm, 10 mm, 8 mm, 5 mm, 3 mm and 1 mm. The crack had a thickness of 1 mm, which is considered quite large for concrete, with usual cracks ranging between 0.1 and 0.4 mm. Preliminary simulations have shown that width of 0.5 mm still results in exactly the same results. It seems that the most important parameter is the healthy remaining cross-section, which does not depend on the width of crack. This has also been studied in other recent studies [2]. Fig. 8a shows the displacement field for the intact specimen

20 μs after the excitation of one cycle of 100 kHz. Fig. 8b shows the waveforms obtained after the completion of the simulation of this case. The characteristic Rayleigh cycle can be distinguished for both receivers. In the case of the second receiver, the initial longitudinal arrivals are clearly seen before the Rayleigh cycle since there is sufficient path for the individual modes to be separated due to different velocities.

In Fig. 8c the case of a subsurface crack, 3 mm below the surface is depicted, while the corresponding waveforms are included in Fig. 8d. Since the crack is close to the surface only a small amount of energy can propagate towards the second receiver. The displacement field is distorted while the waveform of the second receiver is much lower in amplitude since most of the energy is reflected back by the discontinuity. This is also the reason for the large peaks seen between 30 and 60 μs at the waveform of the first receiver. In any case the Rayleigh contribution is clear on both receivers which enables velocity measurements.

In order to study the wavelength influence, the frequency was varied. The change of frequency modifies also the depth of Rayleigh penetration. Three basic cases were examined, namely 100 kHz (similar to the experiment), 200 kHz and 20 kHz. The corresponding Rayleigh wavelengths were 23.2 mm, 11.6 mm and 116.2 mm.

P-wave velocity did not prove sensitive enough to the subsurface damage. For crack 1 mm below the surface the velocity decreases only by 1% for 100 and 200 kHz while for 20 kHz it reduces by 2%, as seen in Fig. 9a. The diagram is in dimensionless form with the velocity of sound material at 4316 m/s. For cracks deeper than 3 mm the velocities are not influenced showing that the narrow surface layer is enough for longitudinal waves to propagate without delay even for the longitudinal wavelength of 216 mm at 20 kHz. This should be stressed out when pulse velocities are measured on the surface of structures with common equipment. This velocity is characteristic only of a very shallow path and any correlation with damage or strength holds for just a few mm of the material under the surface almost independent of frequency.

Concerning Rayleigh waves their velocity is more clearly influenced. For any frequency, as the depth of damage increases, the velocity rises towards the intact material level (2345 m/s).
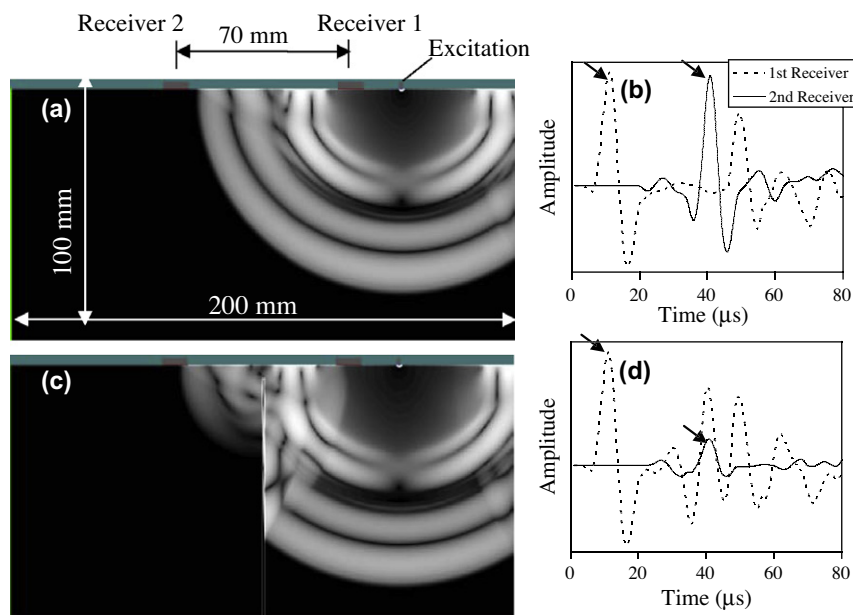

Fig. 8. (a) and (c) Snapshot of the numerically simulated displacement field amplitude for an intact specimen and specimen with a subsurface crack 3 mm below the surface respectively, (b) and (d) waveforms obtained for the simulation of (a) and (c). The frequency is 100 kHz and the arrows in (b) and (d) indicate the strong peaks used for Rayleigh velocity measurements.
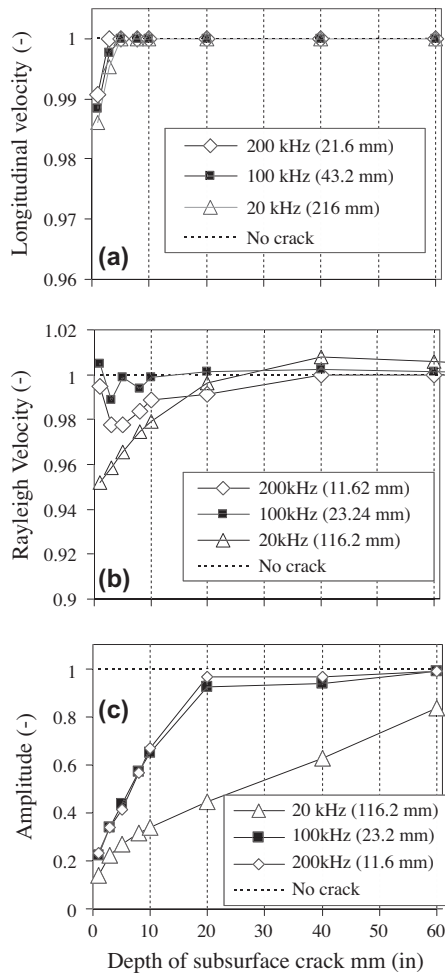
Fig. 9. Longitudinal velocity (a), Rayleigh velocity (b) and amplitude (c) vs. depth to subsurface crack (The number in parenthesis correspond to the wavelength. The values are normalized by those of the uncracked material.).

However, the frequencies of 100 kHz and 200 kHz do not yield a monotonic curve according to the depth to crack (see Fig. 9b). The low frequency of 20 kHz shows a monotonic trend, since the velocity is reduced continuously as the crack gets closer to the surface (5% for crack embedded 1 mm beneath the surface. For the case of deeper position of damage (10 mm from the surface) the Rayleigh velocity is decreased by 2%. This shows that lower frequencies are more reliable since their velocity decreases more clearly for near-surface damage.

In Fig. 9c the amplitude of the second receiver's waveform for different depths of crack is depicted normalized to the amplitude of the second receiver for sound material. It is obvious that the amplitude decreases much more than velocity, especially for very shallow cracks reaching approximately a decrease of 80% compared to the sound case. As the healthy part above the crack increases, quickly the amplitude of the 100 and 200 kHz waves is restored to the reference level, meaning that these frequencies lose their sensitivity for deeper cracks. However, the amplitude of 20 kHz shows a slow rate of increase until even the subsurface crack of 60 mm depth. The amplitude vs. depth line can be roughly considered linear, showing that a positive estimation may be conducted based on the amplitude of the wave which proves to be the most sensitive parameter in order to characterize the depth of the crack. Simulation for deeper cases was not conducted since the cracks considered in this case, originate from metal rebars embedded at approximately 50–60 mm below the surface.

7. Conclusion

This study concerns the characterization of non-visible subsurface damage in concrete. For the specific case of thin crack which propagates radially away from the rebar, the orientation is mainly vertical to the surface. Therefore, the proposed methodology could be used complementary to impact-echo and Ground Penetrating Radar which are specialized to the parallel orientation or defects (like delaminations). One-sided elastic wave measurements were conducted on SFR concrete specimens with subsurface cracks. The basic conclusions are the following:

1. Steel fibers only slightly influence the wave measurements on sound material and therefore do not mask the examination for cracks.
2. Longitudinal and Rayleigh wave velocities decreased by about 25% for the specimens with subsurface cracks.
3. The experimental scatter of the measurement population is more sensitive to the existence of damage, since the crack increases the inhomogeneity of the medium. For damaged concrete, COV increases by more than 300% compared to the sound material. Therefore, it is suggested that a sufficient number of measurements should be conducted in order to examine their standard deviation which is sensitive to damage.
4. The waveform amplitude proved also much more sensitive to damage than velocity, decreasing by about 90% when cracks exist below the surface.
5. Numerical simulations show that subsurface damage is invisible to P-wave velocity even at the depth of 3 mm. The velocity of the Rayleigh is more sensitive and especially for the low frequency of 20 kHz.
6. In order to go one step further from detection, to the characterization of the depth of the crack, the most promising parameter is the amplitude of low frequency waves, which shows a steady decrease as the cracks reaches the surface.

Future steps include the experimental ultrasonic measurements on specimens with different depth of subsurface cracks which will be produced by different deflection at the 4-point bending experiment. Since simulations suggest better capacity by lower frequencies, the use of adequate equipment (e.g. low frequency accelerometers) is proposed. Also, in order to be applied in large concrete surfaces, the specific point of measurement should be selected by another technique of global monitoring. This could be by low frequency Rayleigh wave scanning of the surface [23] or by infrared thermography, which is currently being studied for the detection of thin subsurface cracks at realistic temperatures up to 50 °C [24]. Thermography enables the scanning of a large surface highlighting the points where the subsurface damage leaves its thermal signature. Consequently, one-sided ultrasound can be applied at the specific position for more accurate characterization of damage depth.

Acknowledgements

References

[1] Sansalone MJ, Streett WB. Impact-echo nondestructive evaluation of concrete and masonry. Ithaca, N.Y: Bullbrier Press; 1997.
[2] Aggelis DG, Shiotani T, Polyzos D. Characterization of surface crack depth and repair evaluation using Rayleigh waves. Cem Concr Compos 2009;31(1):77–83.
[3] Tomoda Y, Ohtsu M. Corrosion process of steel bar in reinforced concrete by acoustic emission. Prog Acoust Emission XIV 2008:341–6.

[4] Shiotani T, Aggelis DG, Makishima O. Global monitoring of large concrete structures by acoustic emission and ultrasonic techniques: case study. J Bridge Eng (ASCE) 2009;14(3):188–92.

[5] Qixian L, Bungey JH. Using compression wave ultrasonic transducers to measure the velocity of surface waves and hence determine dynamic modulus of elasticity for concrete. Constr Build Mater 1996;4(10):237–42.

[6] Liu S-W, Sung J-C, Chang C-S. Transient scattering of Rayleigh waves by surface-breaking and sub-surface cracks. Int J Eng Sci 1996;34(9):1059–75.

[7] Hevin G, Abraham O, Pedersen HA, Campillo M. Characterisation of surface cracks with Rayleigh waves: a numerical model. NDT E Int 1998;31(4):289–97.

[8] Zerwer A, Polak MA, Santamarina JC. Rayleigh wave propagation for detection of near surface discontinuities: finite element modelling. J Nondestr Eval 2003:39–52.

[9] Liu SW, Sung JC, Chang CS. Transient scattering of Rayleigh waves by surface-breaking and sub-surface cracks. Int J Eng Sci 1996;34(9):1059–75.

[10] Baron C, Shuvalov AL, Poncelet O. Impact of localized inhomogeneity on the surface-wave velocity and bulk-wave reflection in solids. Ultrasonics 2007;46:1–12.

[11] Divena PS, Manolis GD, Rangelov TV. Sub-surface crack in an inhomogeneous half-plane: wave scattering phenomena by BEM. Eng Anal Boundary Elem 2006;30:350–62.

[12] Soulioti DV, Barkoula NM, Paipetis A, Matikas TE. Effects of Fibre Geometry and Volume Fraction on the Flexural Behaviour of Steel-Fibre Reinforced Concrete. Strain 2011;47:e535–41.

[13] Aggelis DG, Shiotani T. Repair evaluation of concrete cracks using surface and through-transmission wave measurements. Cem Concr Compos 2007;29(9):700–11.

[14] Graff KF. Wave motion in elastic solids. New York: Dover Publications; 1975.

[15] Owino JO, Jacobs LJ. Attenuation measurements in cement-based materials using laser ultrasonics. J Eng Mech (ASCE) 1999(1256):637–47.

[16] Anson LW, Chivers RC. Ultrasonic velocity in suspensions of solids in solids – a comparison of theory and experiment. J Phys D 1993;26:1566–75.

[17] Pecorari C. Scattering of a Rayleigh wave by a surface-breaking crack with faces in partial contact. Wave Motion 2001;33:259–70.

[18] Aggelis DG, Shiotani T. Experimental study of surface wave propagation in strongly heterogeneous media. J Acoust Soc Am 2007;122(5):151–7. EL.

[19] Popovics S, Popovics JS. Effect of stresses on the ultrasonic pulse velocity in concrete. Mater Struct 1991;24(1):15–23.

[20] Jacobs LJ, Owino JO. Effect of aggregate size on attenuation of Rayleigh surface waves in cement-based materials. J Eng Mech ASCE 2000;126(11):1124–30.

[21] Wave 2000, Cyber-Logic, Inc, NY <http://www.cyberlogic.org/>.

[22] Aggelis DG, Momoki S. Numerical simulation of wave propagation in mortar with inhomogeneities. ACI Mater J 2009;106(1):59–63.

[23] Aggelis DG, Momoki S, Chai HK. Surface wave dispersion in large concrete structures. NDT E Int 2009;42:304–7.

[24] Aggelis DG, Kordatos E, Soulioti DV, Matikas TE. Combined use of thermography and ultrasound for the characterization of subsurface cracks in concrete. Constr Build Mater 2010;24:1888–97.